Journal of Environmental Management 303 (2022) 114192

Contents lists available at ScienceDirect

Journal of Environmental Management

journal homepage: www.elsevier.com/locate/jenvman

A designed moderately thermophilic consortia with a better performance for leaching high grade fine lead-zinc sulfide ore

Siyu Zhou [a], Xiaojian Liao [a], Shoupeng Li [a], Xiaodi Fang [a], Zhijie Guan [a], Maoyou Ye [c], Shuiyu Sun [a,b,*]

[a] Guangzhou Key Laboratory Environmental Catalysis and Pollution Control, Guangdong Key Laboratory of Environmental Catalysis and Health Risk Control, School of Environmental Science and Engineering, Institute of Environmental Health and Pollution Control, Guangdong University of Technology, Guangzhou, 510006, China
[b] Guangdong Polytechnic of Environmental Protection Engineering, Foshan, 528216, China
[c] College of Resources and Environment, Zhongkai University of Agriculture and Engineering, Guangzhou, 510225, China

ARTICLE INFO

Keywords:
Bioleaching
Fine particle size raw ore
EPS fraction
Sulfobacillus benefaciens

ABSTRACT

Unwieldy fine sulfide ores are produced during mining; without being appropriately disposed of, they can cause environmental pollution and waste resources. This study investigated the leaching performance of a moderately thermophilic consortia (*Leptospirillum ferriphilum* + *Acidithiobacillus caldus* + *Sulfobacillus benefaciens*) for fine lead-zinc sulfide raw ore. The results showed this microbial community created a low pH, high ORP, and high cell concentration environment for mineral leaching, improving bioleaching efficiency. Under the action of this consortia, the zinc leaching rate reached 96.44 in 8 days, and reached 100% after 12 days. EPS analysis indicated that the consortia could mediate the secretion of more polysaccharides to ensure leaching efficiency. EPS levels and amino acids were the main factors affecting bioleaching. An analysis of mineral surface characteristics showed the consortia effectively leached pyrite and sphalerite from the fine sulfide ore, and prevented the mineral surface forming the jarosite that could hinder bioleaching. This study found that bioleaching reduced the potential environmental toxicity of the minerals, providing an important reference for guiding the bioleaching of unwieldy fine sulfide raw ore.

1. Introduction

Over-grinding and secondary processes occur during mining, generating large amounts of fine sulfide ore. Compared with traditional foam-floatable minerals (at approximately 40 μm or larger), fine sulfide ore has a small mass, large specific surface area, and high activation energy (Mikhlin et al., 2016). This makes it difficult to utilize the fine sulfide raw ore, because it creates a series of problems for mineral concentration, sedimentation, and sorting; and makes it difficult to efficiently recover metal using flotation (Xue et al., 2021). In addition, common tailings treatments have been used to treat fine sulfide ore, causing them to be entered into tailings dumps. This has resulted in the loss of large amounts of valuable metals, along with fine particle ores. Further, this treatment occupies a large treatment area, and produces acid through oxidation. Heavy metal ions then easily migrate, possibly polluting the surrounding environment. Therefore, developing comprehensive technology for utilizing fine sulfide ore is a significant step in protecting the environment, rationally using resources, and promoting economic development.

Compared with physical and chemical methods, bioleaching has been widely used to treat a variety of sulfide ores, because of its environmental friendliness, simple operation, strong oxidation ability, and low cost (Gu et al., 2018; Srichandan et al., 2019). Bioleaching has been investigated as a method for recovering valuable metals from pyrite (Yin et al., 2020), chalcopyrite (Panda et al., 2015), lead-zinc ore (Liao et al., 2021), uranium ore (Kaksonen et al., 2020) and other minerals. More than 40 microbial species with leaching capabilities have been found in bioleaching systems (Panda et al., 2015). Based on their functional categories, acidophilic microorganisms can be divided into ferrous/-sulfur oxidizers, ferrous oxidizers, and sulfur oxidizers (Mendez-Garcia et al., 2015). Acidophiles are further divided into three groups according to their suitable growth temperature: mesophilic (20–40 °C), moderately thermophilic (40–60 °C), and extremely thermophilic (above 60 °C) (Mahmoud et al., 2017). The oxidation of sulfide ore is an

* Corresponding author. School of Environmental Science and Engineering, Guangdong University of Technology, No. 100 Waihuan Xi Road, Guangzhou Higher Education Mega Center, Guangzhou, Guangdong, China.
E-mail address: sysun@gdut.edu.cn (S. Sun).

https://doi.org/10.1016/j.jenvman.2021.114192
Received 21 July 2021; Received in revised form 22 November 2021; Accepted 25 November 2021
Available online 30 November 2021

exothermic reaction, causing the temperature of the leaching system to rise to 50 °C or higher (Zhu et al., 2013). Moderately thermophilic bacteria (40–60 °C) have a strong oxidation capacity and high survivability under adverse conditions. This leads them to perform better compared to mesophilic organisms (20–40 °C) (Castro et al., 2019), which are mostly used in bioleaching. However, long leaching cycles are a problem during bioleaching; and studies have found that bioleaching required approximately 20 days to reach a high metal removal rate (Nguyen et al., 2021). This highlights the need to significantly increase bioleaching efficiency.

Studies have shown that the synergistic effect of different microbial functional types can contribute to the higher metabolism of iron and sulfur, further improving extraction efficiency compared to a pure culture (Ma et al., 2017). The ferrous oxidizer *Leptospirillum* Spp and sulfur oxidizer *Acidithiobacillus* Spp are dominant moderately thermophilic bacteria that have been found in leaching systems (Mahmoud et al., 2017). *Leptospirillum ferriphilum* may have become dominant by oxidizing pyrite to obtain energy for growth (Wang et al., 2018a). However, ferrous oxidizer does not eliminate the sulfur passivation layer formed on the mineral surface, which hinders bioleaching (Liao et al., 2019). Further, the sulfur oxidizer *Acidithiobacillus caldus* may transform sulfide to sulfite, producing acid that further dissolves minerals and avoids the formation of a passivation layer (Mangold et al., 2011). Introducing *Sulfobacillus* Spp can change the community structure to ensure the functioning of dominant bacteria during leaching, benefitting the bioleaching process (Bryan et al., 2011; Nancucheo and Johnson, 2010). Therefore, three types of bioleaching microorganisms described above were selected to construct moderately thermophilic consortia, with the goal of improving the leaching of fine lead-zinc sulfide raw ore.

Extracellular polymeric substances (EPS) serve as a significant medium for the interaction between microorganisms and minerals, and can promote biofilm formation. The biofilm that forms on cell and mineral surfaces provides a reaction site for mineral dissolution and cell energy metabolism, playing an essential role during bioleaching (He et al., 2014; Priya and Hait, 2018). Microbial-mediated EPS can be divided into soluble EPS (S-EPS) and bound EPS (B-EPS); B-EPS is further divided into loosely bound EPS (LB-EPS) and tightly bound EPS (TB-EPS) (Zhang et al., 2019). Studies have shown that the components and structural characteristics of EPS can significantly impact the bioleaching process (Cai et al., 2018; Wang et al., 2018b). Liao et al. (2019) first studied bioleaching with *Leptospirillum ferriphilum* and *Acidithiobacillus thiooxidans* at 30 °C; they developed an EPS extraction method to facilitate an analysis using 3DEEM-PARAFAC. Ye et al. (2021) analyzed the correlation between variations in LB-EPS and TB-EPS and leaching behavior during bioleaching; they confirmed that EPS composition was related to the metal leaching rate. However, few studies have examined characteristic variations of EPS in the process of fine sulfide lead-zinc raw ore bioleaching. Analyzing the characteristic variations in EPS may help reveal the leaching mechanism.

This study focused on assessing the leaching performance of a designed moderately thermophilic consortia. The research also identified the action and mechanism involved in the leaching of fine lead-zinc sulfide raw ore, by examining the bioleaching parameters in the solution, mineral surface characteristics, and EPS characteristics. In addition, the study analyzed the relationship between EPS and leaching behavior using a Pearson correlation. This analysis of the action mechanism was used to analyze the relationship between microbial behavior and mineral dissolution mechanisms. Briefly, the study was designed to improve our understanding of bioleaching and the potential for comprehensively using fine sulfide raw ore from mining.

2. Materials and methods

2.1. Mineral component and characteristics

For this research, fine lead-zinc sulfide raw ore was collected in Shaoguan City in Guangdong Province, China. The XRD result indicated that the fine lead-zinc sulfide raw ore mainly consisted of pyrite, quartz, calcite, sphalerite, and galena. Samples were digested in a microwave (MARS6, CEM, United States). Then, the Fe and Zn concentrations were determined using ICP-OES (7500, Agilent, United States). The sulfur concentrations were detected using an elemental analyzer (Vario EL cube, Elemantar, Germany). Particle size distributions were measured with a laser diffraction particle size analyzer (Mastersizer 3000, Malven, United Kingdom). The results are shown in Table 1.

2.2. Microorganisms cultivation and domestication

Three typical bioleaching strains were used in this research, based on their different energy utilization types. The ferrous oxidizer *L. ferriphilum* DX-m, sulfur oxidizer *A. caldus* DSM 8584T, and ferrous/sulfur oxidizer *S. benefaciens* DSM 2705T were provided by Key Lab of Bio-hydrometallurgy of Ministry of Education, Central South University. The microbial culture conditions are provided in Table 2. The *L. ferriphilum*, *A. caldus* and *S. benefaciens* were grown as pure cultures in a 9K basal medium containing 0.50 g/L $MgSO_4{\cdot}7H_2O$, 0.10 g/L KCl, 3.00 g/L $(NH_4)_2SO_4$, 0.01 g/L $Ca(NO_3)_2$, and 0.50 g/L K_2HPO_4 at 40 °C conditions. The medium was stirred at 170 rpm. Next, the microorganisms were domesticated, by growing them on mineral pulp. After adapting to the fine lead-zinc sulfide ore, the cell-containing pulp was centrifuged for 7 min to separate the sediment (955×*g*). Then, the supernatant was centrifuged for 20 min to obtain the suspended cells at 10,619×*g*. Fresh 9K basal medium (25 mL) was added to suspend the sediment. Next, 1 g of 0.2 mm glass beads were added, and the sample was exposed to a vortex for at least 5 min to collect the attached cells (Feng et al., 2016). The microorganisms that adhered to the wall of the centrifuge tube were then resuspended in 9K basal medium, and were used as the bacterial materials for experiments.

2.3. Bioleaching experiments

For the bioleaching experiment, 100 mL of the 9K basal medium was added to 250 mL flasks containing 5 g fine lead-zinc sulfide raw ore. These were sterilized by autoclaving. Before inoculation, the initial pH of the pulp was adjusted to 1.8, using 50% H_2SO_4. The sample was bioleached at 40 °C and 170 rpm using an inoculation method, where *L. ferriphilum*+*A. caldus*+*S. benefaciens* were mixed in equal proportions, with a total of 10^7 cells/mL. An abiotic control group was assessed without adding bacteria. The two experimental groups were as follows: (I) raw ore - abiotic; (II) raw ore - bioleaching. During bioleaching, flasks were periodically supplemented with distilled water and the 9K basal medium to mitigate evaporation and sampling loss.

2.4. Analytical methods

2.4.1. Analysis of leaching parameters

In the bioleaching experiment, the pH, ORP value, metal ion concentration, and microbial count were measured once every two days. The ORP and pH were measured several times using an oxidation reduction potential meter, with Ag/AgCl as a reference electrode (STORP1, OHAUS, USA) and a digital pH meter (STARTER 2100, OHAUS, USA). Each sample was filtered through a 0.45 μm filter before measuring the ferric [Fe^{3+}], total iron [TFe], and zinc ion

Table 1
Mineral properties.

Mineral species	Concentration of main element (%)			Particle size (μm)		
	Fe	Zn	S	DV(10)	DV(50)	DV(90)
Fine raw ore	13.93	3.42	17.73	2.18	8.30	30.3

Table 2
The culture conditions of microorganisms used in this study.

Species	Strains	Energy type	Growth requirements		
			pH	Temp (°C)	Media (g/L)
Leptospirillum ferriphilum	Dx-m	Ferrous oxidizer	1.6	40	9K + $FeSO_4$ (44.7)
Acidithiobacillus caldus	DSM 8584T	Sulfur oxidizer	2.5	40	9K + S (10)
Sulfobacillus benefaciens	DSM 2705T	Ferrous/ Sulfur oxidizer	2.5	40	9K + S (10)

concentrations. The ferric ion and total iron concentrations were measured using 5-sulfosalicylic acid spectrophotometry (Liao et al., 2019). The zinc concentration was determined using ICP-OES (720ES, Agilent, USA). The number of suspended cells and attached cells were counted using a binocular biological microscope (B203LED, OPTEC, China) (Feng et al., 2016). The Zeta potential and particle size were determined using a research grade light scattering system (BI-200SM, Brookhaven, USA) and laser diffraction particle size analyzer (Mastersizer 3000, Malven, United Kingdom).

2.4.2. Extraction and analysis of EPS

2.4.2.1. Extraction of EPS during bioleaching process. During the experiment, the bound EPS fractions were extracted from the leaching system of the biological group once every 4 days. This was done using a previously published method for extracting EPS from tailings pulp (Liao et al., 2019). Before analysis, 0.45 μm acetate cellulose membranes were used to filer the EPS layers; the EPS composition and structure were then analyzed.

2.4.2.2. Fluorescence EEM measurement and FRI technique. Each layer of EPS was analyzed using a three-dimensional excitation emission matrix fluorescence spectrophotometer (F-4600, Hitachi, Japan) at a scan speed of 2400 nm/min. The scan range of the emission (Em) spectra ranged from 250 to 500 nm; the excitation (Ex) spectra ranged from 200 to 500 nm. The spectra were recorded at an Em and Ex sampling interval of 5 nm, under identical slit bandwidths (5 nm). Water was used for blank scans at equivalent conditions. The fluorescence intensity of the blank sample was subtracted from the experimental sample to eliminate water Raman scatter peaks (Xu et al., 2013). To determine the variation in EPS components, FRI was used to resolve the EEM data using Origin 96 software (Math Works, Natick, Massachusetts, United States). The fluorescence spectra were decomposed into independent fluorescence components; this allowed for the determination of the maximum fluorescence intensity fraction peak position and other parameters (Han et al., 2018; Xu et al., 2013). The FRI technique was performed to quantify the dissolved organic matter, by quantitatively using all wavelength-dependent fluorescence intensity data in EEMs (Chen et al., 2003). This step involved integrating the volumes within each EEM region.

2.4.2.3. Polysaccharide and DOC of EPS measurement. The polysaccharide concentrations in each EPS layer sample were analyzed using the phenol-sulfuric acid method, using glucose as the standard (Li and Sand, 2017). The levels of dissolved organic carbon (DOC) in the S-EPS, LB-EPS, and TB-EPS were measured using a TOC analyzer (Multi N/C 3100, Analytik Jena, Germany).

2.4.2.4. Correlation analysis of EPS and solution medium. A Pearson correlation analysis was used to evaluate the relationship between the changes in EPS fractions and the bioleaching parameters. Statistical analyses were performed using SPSS (SPSS 22.0; SPSS, Munich, Germany).

2.4.3. Mineral solid phase characteristics

For the final experiment, the leaching residues were freeze-dried in a vacuum at low temperature after being washed in distilled water. The variations in the solid phase of the fine lead-zinc sulfide ore during bioleaching were observed using a Fourier Transform infrared spectroscopy (FTIR) (Nicolet 6700, Thermo-Filsher, USA), X-ray Diffractometer (XRD) (D8 ADVANCE, Bruker, Germany), and scanning electron microscope (SEM) (Sigma300, ZEISS, Germany).

3. Results and discussion

3.1. Variation in the bioleaching parameters

The pH, ORP, [Fe^{3+}], [TFe], microbial count, and zinc extraction rate were investigated to evaluate the leaching performance of fine sulfide lead-zinc raw ore during bioleaching. Fig. 1(a) shows the change in pH during leaching for the different groups. The variations in pH resulted from competition between acid production by microbial oxidation and acid consumption by mineral dissolution. The pH of the abiotic control group remained stable at approximately 1.80, while the biological group experienced a decline in pH as the metal sulfides dissolved. In the adaptive phase (0–4 days), the pH slowly declined, likely due to the weak oxidation capacity of the microorganisms. Subsequently, from days 4–10, there was a rapid decline in pH from 1.80 to approximately 1.13, given that the microbial count rapidly increased. The increase in the microbial count was accompanied by the oxidation of ferrous and sulfide ions. This in turn facilitated the gradual dissolution of fine sulfide ore, as shown in (Eqs. (1)–(7)). Fine sulfide raw ore was characterized as having small particle sizes and a large specific area, providing more active sites for reaction. Therefore, the fine sulfide raw ore was favorable for producing acid during bioleaching compared with ores with larger particle sizes (pH value of 1.13 compared to 2.0 at 10 days) (Ahmadi and Mousavi, 2015). The lower pH value facilitated the dissolution of the fine sulfide ore.

$$4FeS_2 + 4H_2O + 14O_2 \xrightarrow{\text{bacteria}} 4Fe^{2+} + 8SO_4^{2-} + 8H^+ \quad (1)$$

$$MS_{(s)} + 2O_2 \xrightarrow{\text{bacteria}} M^{2+} + SO_4^{2-} \quad (2)$$

$$MS_2 + 2Fe^{3+} \rightarrow M^{2+} + 2Fe^{2+} + 2S^0 \quad (3)$$

Table 3
Analysis of correlations between each EPS component and leaching parameters.

	Polysaccharides	DOC	Protein	Amino acids	Humic acids	Fulvic acids
Zinc extraction rate	0.954*	0.963*	−0.920	−0.994**	0.943	0.060
pH	−0.955**	−0.964*	0.917	0.977*	−0.920	−0.170
ORP	0.958*	0.959*	−0.913	−0.933**	0.949	0.052
Fe^{3+}	0.979*	0.873	−0.797	−0.903	0.915	0.255
TFe	0.904	0.749	−0.658	−0.756	0.792	0.454
Microbial count	0.999**	0.833	−0.749	−0.915	0.981*	0.028

Note: *. The correlation was significant at 0.05 level (2-tailed).
**. The correlation was significant at 0.01 level (2-tailed).

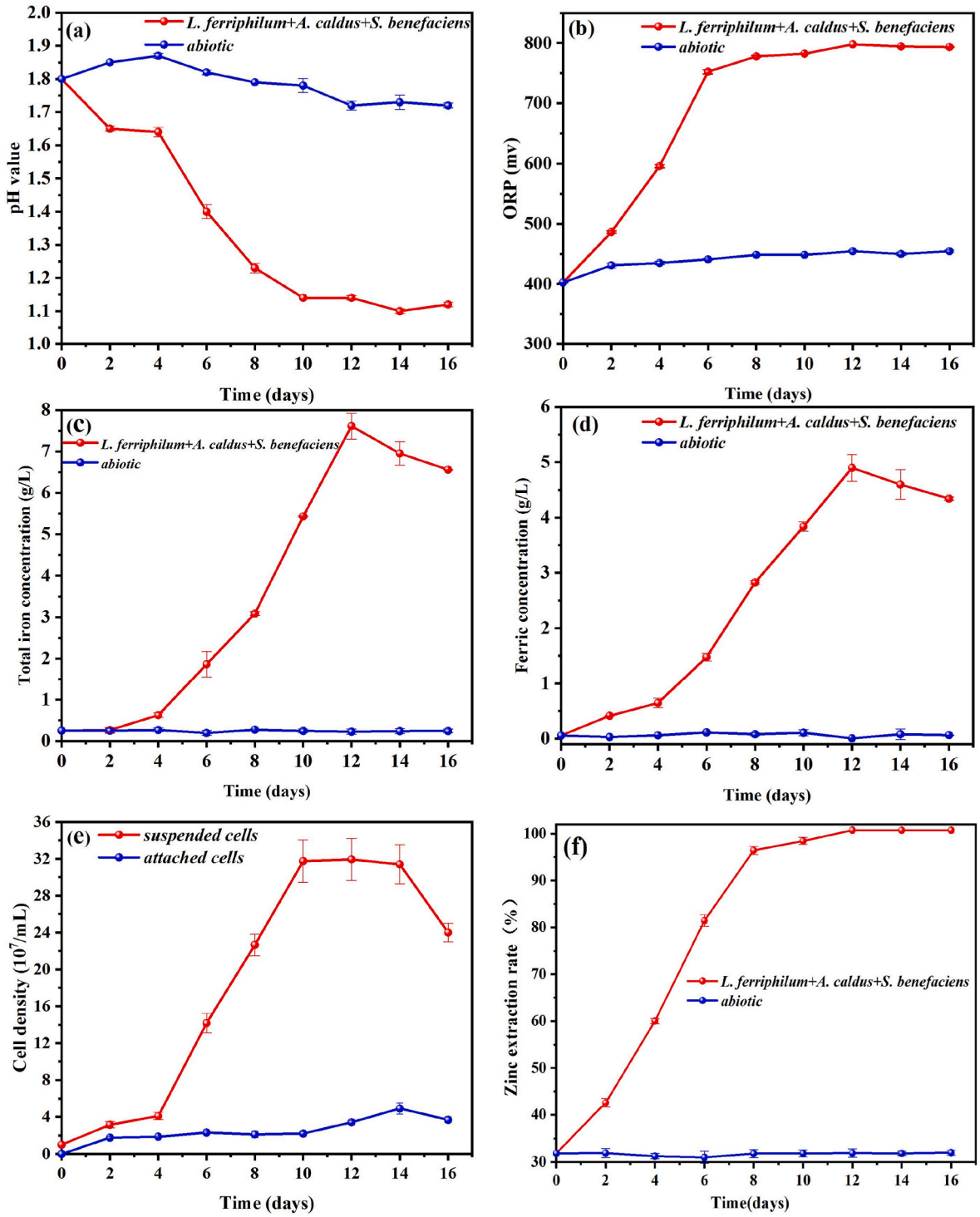

Fig. 1. The variations in media parameters during bioleaching: (a) pH, (b) ORP, (c) total iron concentration, (d) ferric concentration, (e) microbial count, (f) zinc extraction rate.

$$MS + 2Fe^{3+} \rightarrow M^{2+} + 2Fe^{2+} + S^0 \quad (4)$$

$$4Fe^{2+} + O_2 + 4H^+ \xrightarrow{\text{bacteria}} 4Fe^{3+} + 2H_2O \quad (5)$$

$$2S^0 + 3O_2 + 2H_2O \xrightarrow{\text{bacteria}} 4H^+ + SO_4^{2-} \quad (6)$$

$$2ZnS + O_2 + 4H^+ \rightarrow 2Zn^{2+} + 2H_2O + 2S^0 \quad (7)$$

Fig. 1(b)–(d) shows the variations in ORP, [TFe] and [Fe^{3+}] as a result of leaching for the different groups. The ORP value is an important factor reflecting leaching efficiency, and is significantly related to the ratio of [Fe^{3+}] to [Fe^{2+}] (Zhao et al., 2015). In the abiotic group, the ORP, [TFe] and [Fe^{3+}] remained stable; the ORP value remained at approximately 390–400 mv; and [TFe] and [Fe^{3+}] remained at approximately 0.51 g/L and 0.05 g/L, respectively. For the bioleaching of raw ore, the ORP value increased sharply from 389 mv to 799 mv in 8 days, with the enrichment of [TFe] and [Fe^{3+}]. Additionally, [TFe] increased from 0.51 g/L to 3.55 g/L, and [Fe^{3+}] increased from 0.05 g/L

to 2.55 g/L in the biological group.

There are two likely reasons for the increase in ORP. One explanation is that *L. ferriphilum* and *S. benefaciens* directly utilized Fe^{2+}, continuously oxidizing Fe^{2+} to Fe^{3+}, as shown in (Eq. (5)). A second explanation is that *A. caldus*, a sulfur-oxidizer, used sulfur to produce acid, as shown in (Eq. (6)). The efficient use of sulfur benefitted the high redox potential of the bioleaching (Gan et al., 2015). The results show there was an increase in [Fe^{3+}] and a high ORP during bioleaching by the moderately thermophilic consortia. This led to an increase in the oxidation rate of pyrite and sphalerite (Gan et al., 2015; Sun et al., 2015).

The microbial count of moderately thermophilic consortia is an important index in bioleaching, due to the correlation with the leaching rate. An increase in microbial count supports the oxidation of sulfide ore and facilitates metal dissolution. Bioleaching occurs through the combined action of suspended and attached cells. In this study, the dissolved metals continuously increased through the oxidation of growing microorganisms. Fig. 1(e) shows that the microbial count of suspended cells increased slowly in the first 4 days, due to the environmental adaption of microorganisms. During this period, microorganisms gradually adhered to the mineral surface. After 4–10 days, suspended cells continuously obtained energy from the fine sulfide ore to grow and reproduce. The microbial count of suspended cells sharply rose from 4.08×10^7 cells/mL to 3.17×10^8 cells/mL between 4 and 10 days. The attached cells remained at approximately 2.20×10^7 cells/mL. The attachment behavior of microorganisms was limited by mineral particle size; a fine particle size did not benefit the attachment to the mineral surface. Days 10–16 represented the late leaching stage. The total microbial count remained stable at 10–14 days; however, microorganisms began to decline after 14 days, due to a lack of energy. Compared to sulfide tailings with low metal concentrations, microorganisms maintained a higher level of microbial activity when exposed to raw ore with high metal concentrations (total microbial count of 3.39×10^8 cells/mL compared to 2.10×10^8 cells/mL at 10 days) (Liao et al., 2019). These results indicated that the moderately thermophilic consortia (*L. ferriphilum*+*A. caldus*+*S. benefaciens*) showed strong environmental adaptability for fine sulfide lead-zinc ore at high metal concentrations.

In bioleaching, the metal extraction rate is an important index reflecting leaching performance. Fig. 1(f) shows that over 16 days, the zinc extraction rate remained at approximately 31.83% for the abiotic control group. There were significant differences between the biological group and the abiotic group. The zinc extraction rate sharply increased to 96.44% for biological group after 8 days, and then asymptotically reached nearly 100% at 12 days. The results showed a superior zinc extraction rate by the consortia, shortening the required time by 6–42 days, compared to previous research (Liao et al., 2021; Ye et al., 2017a; Zahiri et al., 2021) (Table 4). This increased zinc extraction can be attributed to microbial oxidation (Eq. (2)). Sphalerite was dissolved by ferric ion, but was also found to be an acid-consuming mineral (Eq. (4) and (7)). The zinc extraction rate of nearly 100% was attributed to the lower pH, the higher ORP value and [Fe^{3+}] level, and higher microbial activity level in the biological group. Therefore, using moderately thermophilic consortia (*L. ferriphilum*+*A. caldus*+*S. benefaciens*) bioleaching enabled the efficient recovery Zn from fine lead-zinc sulfide raw ore.

Table 4
Recent bioleaching research.

Microorganism	Time	Leaching rate	Reference
L. ferriphilum, A. caldus and *S. benefaciens*	8 days	96.44%	–
A. ferrooxidans	50 days	96.42%	Ye et al. (2017b)
A. ferrooxidans and S. thermosulfidooxidans	14 days	94.2%	Liao et al. (2021)
A. caldus, Sulfobacillus sp, Ferroplasma sp, and *Leptospirillum sp*	30 days	72.25%	Zahiri et al. (2021)

3.2. The change in the EPS characteristics in bioleaching

To further explore the bioleaching behavior of moderately thermophilic consortia, specifically with respect to variations in the EPS during the leaching process, fluorescence EEM measurement with the FRI technique was used to generate detailed information about the EPS composition (Guo et al., 2014). The 3DEEM fluorescence spectra of biological group are shown in Fig. 2. Based on several studies (Wang and Zhang, 2010; Wei et al., 2017), the 3DEEM fluorescence spectra were divided into 4 regions: Region I (Ex/Em = 275/310 nm) represented tyrosine/tryptophan protein substances; Region II (Ex/Em = 220/310 nm) represented tyrosine/tryptophan substances; Region III (Ex/Em = 290/380 nm) represented humic acid-like substances; and Region IV (Ex/Em = 225/400 nm) represented fulvic acid-like substances. The fluorescence region integration (FRI) of the above-mentioned substances in the EPS is shown in Fig. 3(c)–(f). The appearance and fluorescence intensity of the 4 regions varied during bioleaching.

Fig. 3(a) shows the trend in DOC, which was similar to the Zn extraction rate (Fig. 1(f)). DOC contains carbon from polysaccharides, proteins, humic substances, and other organics from EPS fractions; this can be used to infer the variations in total EPS (Zhao et al., 2019). During days 4–8 of leaching, the total DOC concentrations in the biological group initially increased from 11.48 mg/L to 27.92 mg/L. As the bioleaching continued and the microbial count grew, the increased EPS ensured the nutrient-adsorbing capacity of the biofilm and enabled microbial survival in the unfavorable environment. This was characterized by a lower pH and higher metal ion concentrations (Li and Sand, 2017). There was a slight drop of the total DOC content between day 8 and day 12, followed by an increase in the total DOC concentration from day 12 to day 16. Cell death released intracellular substances, such as DNA, RNA, lipids proteins and polysaccharides (Wong et al., 2015). This explained the increased total DOC during the late stage. Moreover, during the bioleaching process, S-EPS mainly contributed to the DOC, produced by the suspended cells. EPS plays an important role in promoting microbial attachment (Flemming and Wingender, 2010). However, the DOC concentration of B-EPS remained stable at approximately 4.65 mg/L after 4–12 days, with the microbial count of attached cells remaining at approximately 2.20×10^7 cells/mL. The suspended cells mainly produced the EPS available for action during bioleaching.

Fig. 3(b) shows the variation in polysaccharides. During bioleaching, the total polysaccharide levels first increased and then decreased. The S-EPS layer contributed the main component. The polysaccharides level was higher in the S-EPS compared to the B-EPS, because microorganisms secreted polysaccharides into the S-EPS to fight the unfavorable environment of high heavy metal concentrations and a low pH (Yu et al., 2017). When the microorganisms were introduced into the leaching system, polysaccharide production accompanied the proliferation of microorganisms. The polysaccharide levels in the EPS fractions significantly increased from 49.73 mg/L to 390.38 mg/L in the first 12 days. A large number of polysaccharides were seen during bioleaching, and the polysaccharide level changed in a similar way as the microbial count (Fig. 1(e)). Polysaccharides played an important role in bioleaching. First, polysaccharides and protein mainly participated in the EPS matrix structural components, ensuring microbial adhesion (Flemming and Wingender, 2010). Other, polysaccharides complexed Fe^{3+} to create a positive charge and facilitate attachment to the negatively charged mineral surface. This supported the accumulation of a large amount of Fe^{3+} between the mineral surface and the EPS. This effectively promoted the erosion and dissolution of the mineral and enhancing the metals extraction rate (Li and Sand, 2017; Wang et al., 2018b). In the late leaching stage, with the hydrolysis of polysaccharide glucose bonds or lower microbial metabolic capacity (Xiao et al., 2016), the polysaccharide levels declined from 390.38 mg/L to 298.52 mg/L after 12 days. As noted above, the increased polysaccharide promoted the leaching process.

Extracellular proteins played an important role in the oxidation-

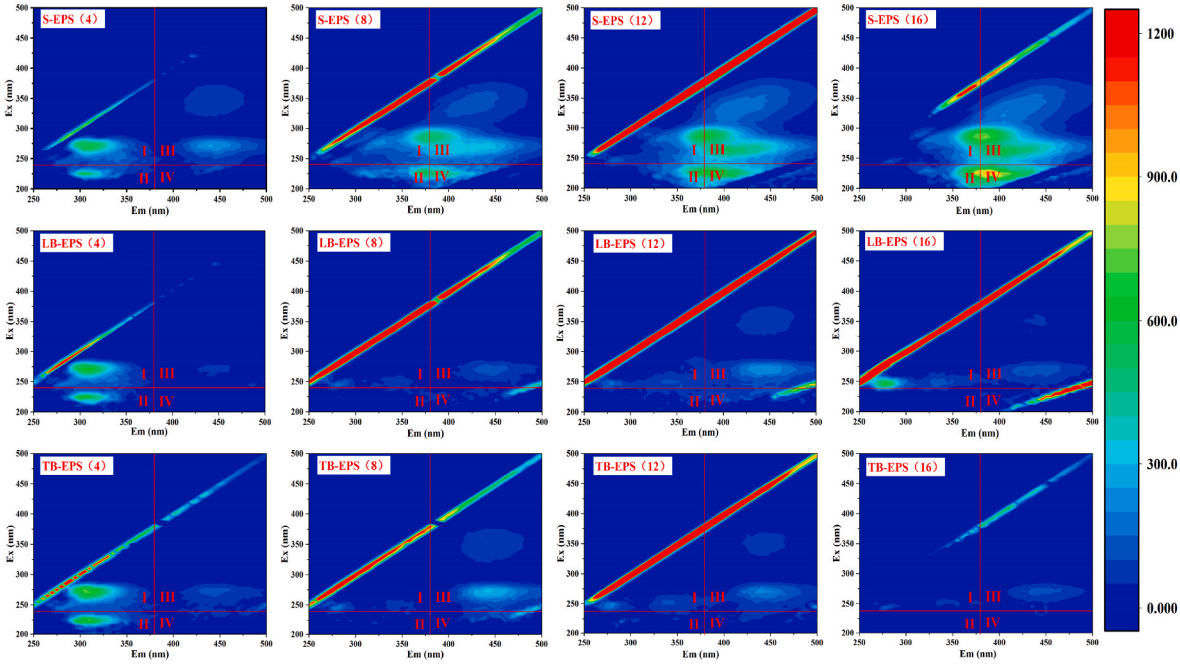

Fig. 2. The 3DEEM fluorescence of each EPS layer at different leaching times for raw ore - bioleaching. (I, II, III, IV represent different fluorescent substance region).

reduction process of EPS biofilm. This ensured the mechanical stability of the biofilm, and facilitated the adhesion between cell-matrix and cells (Flemming and Wingender, 2010). There was a similar trend with respect to the fluorescence intensity for protein-like and amino acid-like substances (Fig. 3(c)–(d)). In the adaptive phase (0–4 days), the fluorescence intensity of protein-like and amino acid-like substances rapidly increased to 3.62×10^6 RU and 0.95×10^6 RU, respectively. Microorganisms adsorbed on the mineral surfaces and adapted to the unfavorable environments following secretion of protein-like substances and extracellular enzymes (Liao et al., 2019). However, the fluorescence intensity of protein-like and amino acid-like substances sharply declined to 2.12×10^6 RU and 0.29×10^6 RU, respectively, at 12 days. Therefore, the secretion of protein-like and amino acid-like substances mainly played an important role in the adaptive phase of bioleaching. After that, with the decline in total microbial count, the secretion of proteins further decreased at 16 days.

Humic substances complexed with metal ions and modified the speciation of metals through oxidation reduction reactions; this played an important role in bioleaching (Castro et al., 2013). Fig. 3(e) shows that the S-EPS layer contributed the main component, indicating that suspended cells play a major role in producing humic acid. The humic acid level first rose and later fell. The fluorescence intensity of humic acids increased continuously, from 3.38×10^5 RU to 7.17×10^5 RU within 12 days. The increase in dissolved metal ions during bioleaching resulted in the accumulation of humic acid-like substances (Ye et al., 2021). This occurred because humic acids and metal ions combined, affecting the transfer and transformation of metals, and protecting the microorganisms (Koukal et al., 2003). Further, humic acid substances form stable complexes with extracellular enzymes, and are highly resistant to heat changes, dehydration, and the hydrolysis of proteins. In addition, they act as a communication medium between minerals and microorganisms, significantly affecting electron transfer between extracellular electron acceptors and microorganisms (Koukal et al., 2003; Xiao et al., 2019). However, from 12 to 16 days, the fluorescence intensity for humic acids slightly decreased, from 7.17×10^5 RU to 5.85×10^5 RU. This decrease may be attributed to the increased degradation of dead microorganisms from the fine sulfide lead-zinc ore bioleaching (Ye et al., 2021).

In the first 4 days, a large of fulvic acids were produced due to their initial exposure to the unsuitable environment of fine sulfide raw ore (Chu et al., 2021). The fluorescence intensity of fulvic acid-like substances rapidly increased to 1.22×10^6 RU (Fig. 3(f)). After that, the intensity sharply declined to 0.28×10^6 RU in 8 days. Finally, the fluorescence intensity continuously increased to 2.14×10^6 RU in 16 days. The increased fulvic acids may have separated and released iron from the mineral surfaces into the water phase, by forming a fulvic acid-iron complex or through reduction (Xie et al., 2017). At the same time, fulvic acids can also complex with other metals, such as lead (Novikova and Gas'kova, 2013). However, as the heavy metal levels increased in the solution, fulvic acid production increased.

The EPS fractions changed in different ways during bioleaching. However, the suspended cells were the main driver for producing EPS fractions, which was limited by fine particle size. In the early stage, the environmental adaption capacity of moderately thermophilic consortia promoted the production of more protein-like, amino acid-like substances, and fulvic acid-like substances. As the bioleaching process proceeded, the EPS content, polysaccharides, and humic acids gradually increased to ensure bioleaching. These outcomes were correlated with the variation of bioleaching parameters, which facilitated the leaching of metals.

3.3. Correlation analysis of EPS and bioleaching performances

Bioleaching is a dynamic process involving constant changes; the EPS components also vary during the process. As such, a Pearson correlation analysis was conducted to further determine the relationship between EPS components and fine sulfide ore bioleaching performance. Table 3 shows that polysaccharides, DOC, and the amino acids of EPS fractions were strongly correlated with bioleaching performance.

The data in Table 3 show that polysaccharides were strongly correlated with microbial count and pH ($R = 0.999$, -0.955, respectively, $p < 0.01$). The Pearson's correlation coefficient between the polysaccharide levels and the zinc extraction rate, ORP, and $[Fe^{3+}]$ were 0.954, 0.958 and 0.979, respectively, ($p < 0.05$). The polysaccharide levels were significantly correlated with fine sulfide lead-zinc ore bioleaching performance. DOC was also highly correlated with bioleaching performance. The Pearson's correlation coefficient between DOC and the pH and ORP levels were -0.964 and 0.959 respectively, ($p < 0.05$); the

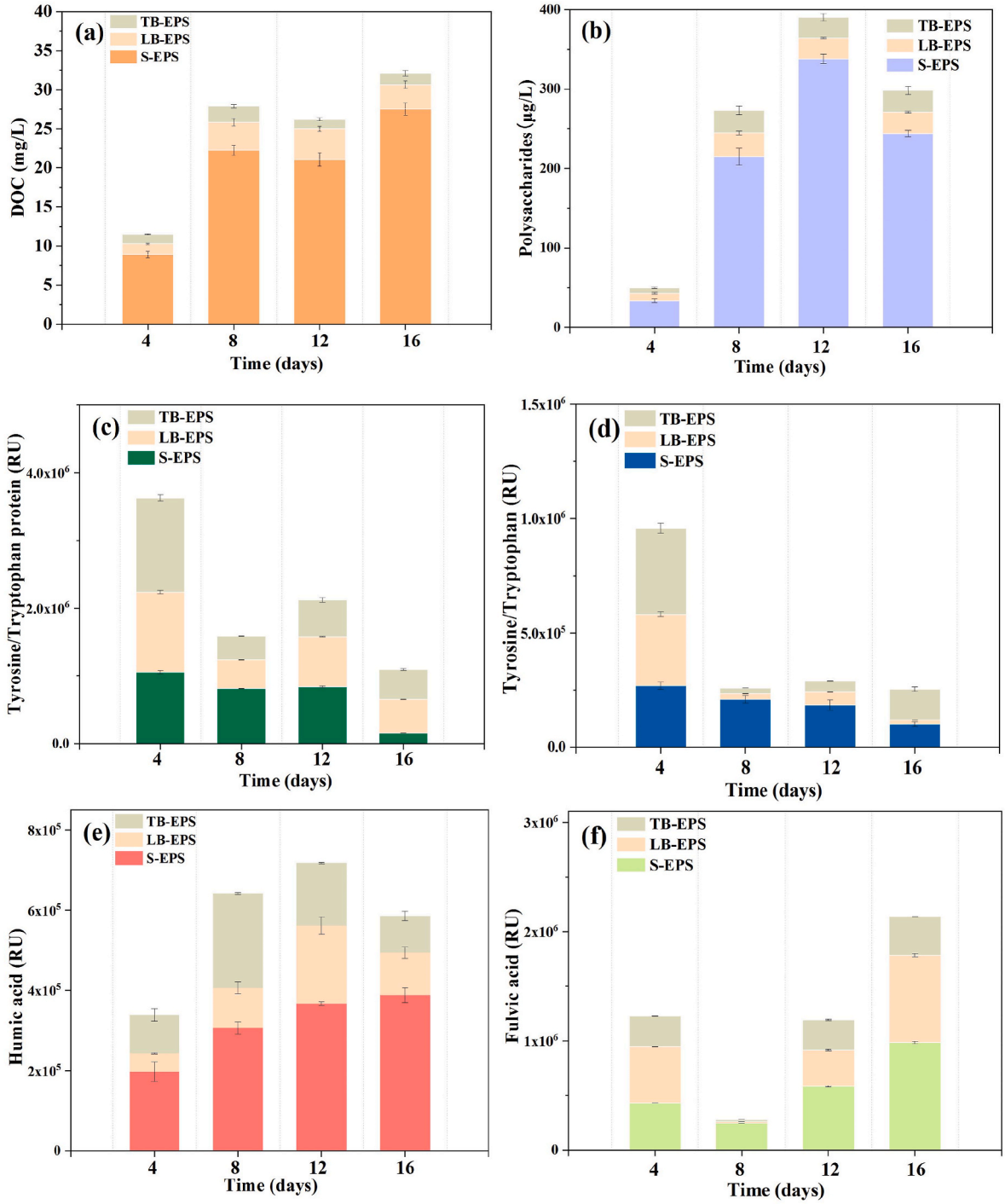

Fig. 3. The variation in the organic matter in the EPS. (a) DOC, (b) Polysaccharides, (c) Tyrosine/Tryptophan protein, (d) Tyrosine/Tryptophan, (e) Humic acid, (f) Fulvic acid.

correlation with the zinc extraction rate was 0.963, ($p < 0.05$). There was a highly significant correlation between amino acids and bioleaching performance. Amino acids were strongly negatively correlated with the zinc extraction rate and ORP ($R = -0.994$ and -0.933, respectively, $p < 0.01$), and were positively correlated with pH ($R = 0.977$, $p < 0.05$). However, there were few significant correlations among protein, humic acid, and leaching parameters; the absolute value of the correlation coefficients were above 0.6, ($|R| > 0.6, p > 0.05$). The absolute value of the correlation coefficient between fulvic acids and leaching parameters were below 0.5, ($|R| < 0.5, p > 0.05$).

Overall, these results indicate that polysaccharides, DOC, and amino acids of the EPS fractions were strongly correlated with bioleaching performance, compared with protein, humic acid, and fulvic acids. This result further reveals that polysaccharides, DOC, and amino acids played significant roles during fine sulfide ore bioleaching.

3.4. Variations in the mineral surface characteristics

3.4.1. FTIR analysis of fine sulfide lead-zinc ore

Fig. 4(a) identifies the FTIR spectrum of the fine sulfide ore during bioleaching. FTIR analysis shows that the peaks at 600 and 3560 cm^{-1} during the bioleaching of the sample represented gypsum; the change in

absorbance frequency was attributed to the calcite reacting with sulfate to form gypsum (Ye et al., 2017b). The strong infrared absorption peak of SO_4^{2-} at 670 cm^{-1} indicated continuous oxidation to sulfate (Liu et al., 2020). Peaks were also observed at approximately 1000–1200 cm^{-1}, which were assigned to C–O–C and C–O, and which corresponded to the presence of carbohydrates (Jiang et al., 2012). The change at 1130 cm^{-1} represented the change in polysaccharides (Wang et al., 2018b). Polysaccharides were produced on the mineral surface during bioleaching, which corresponded with the trend in EPS fractions (Fig. 3 (b)). During bioleaching, a broad stretching vibration at 1620-1680 cm^{-1} and 3400 cm^{-1} related to the characteristic absorption bands of gypsum (Huang et al., 2019; Ye et al., 2017b). The absorption peak at 2400 cm^{-1} is generally closely associated with jarosite (Feng et al., 2021), but jarosite was not created during the bioleaching of fine sulfide ore. Adding moderately thermophilic consortia inhibited jarosite formation, and these results confirm that no jarosite was formed during bioleaching. In contrast, polysaccharides were found on the mineral surface, which benefitted bioleaching.

3.4.2. Surface charge analysis of fine sulfide lead-zinc ore

Fig. 4(c) shows the surface charge characteristics of the fine sulfide lead-zinc ore. The figure shows that the zeta potential rose sharply from −10.96 mV to 7.08 mV in 2 days. The surface charge of fine sulfide lead-zinc ore then remained positive and stable after 2 days. The variation in the zeta potentials occurred in the same order as the count of attached microbes on the fine sulfide lead–zinc ore. The FTIR and zeta potential results indicate that the surface charge remained positive during bioleaching due to a complex of polysaccharides and Fe^{3+}, supporting the leaching process (Zhu et al., 2015).

3.4.3. XRD analysis of fine sulfide lead-zinc ore

XRD spectra revealed that the fine lead-zinc sulfide ore mainly consisted of pyrite, quartz, calcite, sphalerite, and galena (Fig. 4(b)). After bioleaching, the absorption peaks of pyrite, quartz, calcite, sphalerite, galena in mineral residues weakened, while new absorption peaks appeared. Jarosite did not appear to be formed by pyrite dissolution. The microorganisms continuously oxidized the pyrite, sphalerite, and galena in the mineral, generated a large number of ferric and sulfate ions to dissolve the sulfide ore, and facilitated metals dissolution. Finally, when the pyrite, sphalerite, and galena diffraction peak disappeared, the calcite further reacted with sulfate to form gypsum. There was also a strong diffraction peak representing anglesite in bioleaching residues, which was attributed to the lead released from galena, which reacted with sulfate to become anglesite.

3.4.4. SEM analysis of fine sulfide lead-zinc ore

SEM images were used to observe the mineral surface morphology during bioleaching (Fig. 5(a)–(e)). The figure shows that, at first, the fine sulfide ore surface was smooth, with no evident fragments. As bioleaching progressed, the mineral surface gradually appeared to be slightly corroded, with a few fragments in the early stage. This was due to the cycle of Fe^{2+}- Fe^{3+} attachment and the continuous oxidation of minerals under the microbial action, and continuous acid production to oxidize elemental sulfur. As biological oxidation proceeded, the mineral surface gradually became rough, and a fragment mass emerged after 8 days. The smaller fine ores appeared to be clustered at the bigger fine

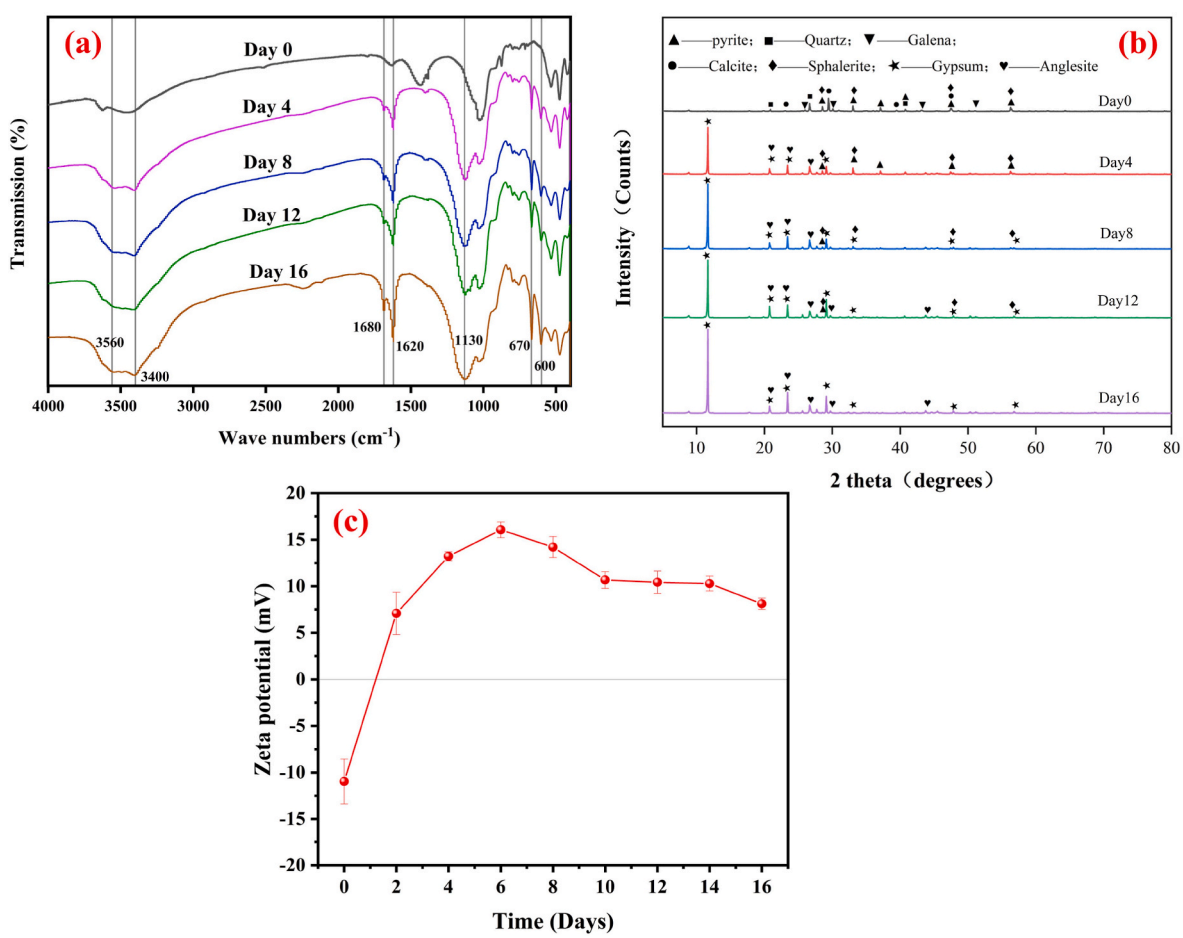

Fig. 4. (a) The FTIR of fine sulfide raw ore during bioleaching, (b) XRD spectrograms of fine sulfide raw ore at different leaching times, (c) Zeta potential variation with different leaching time.

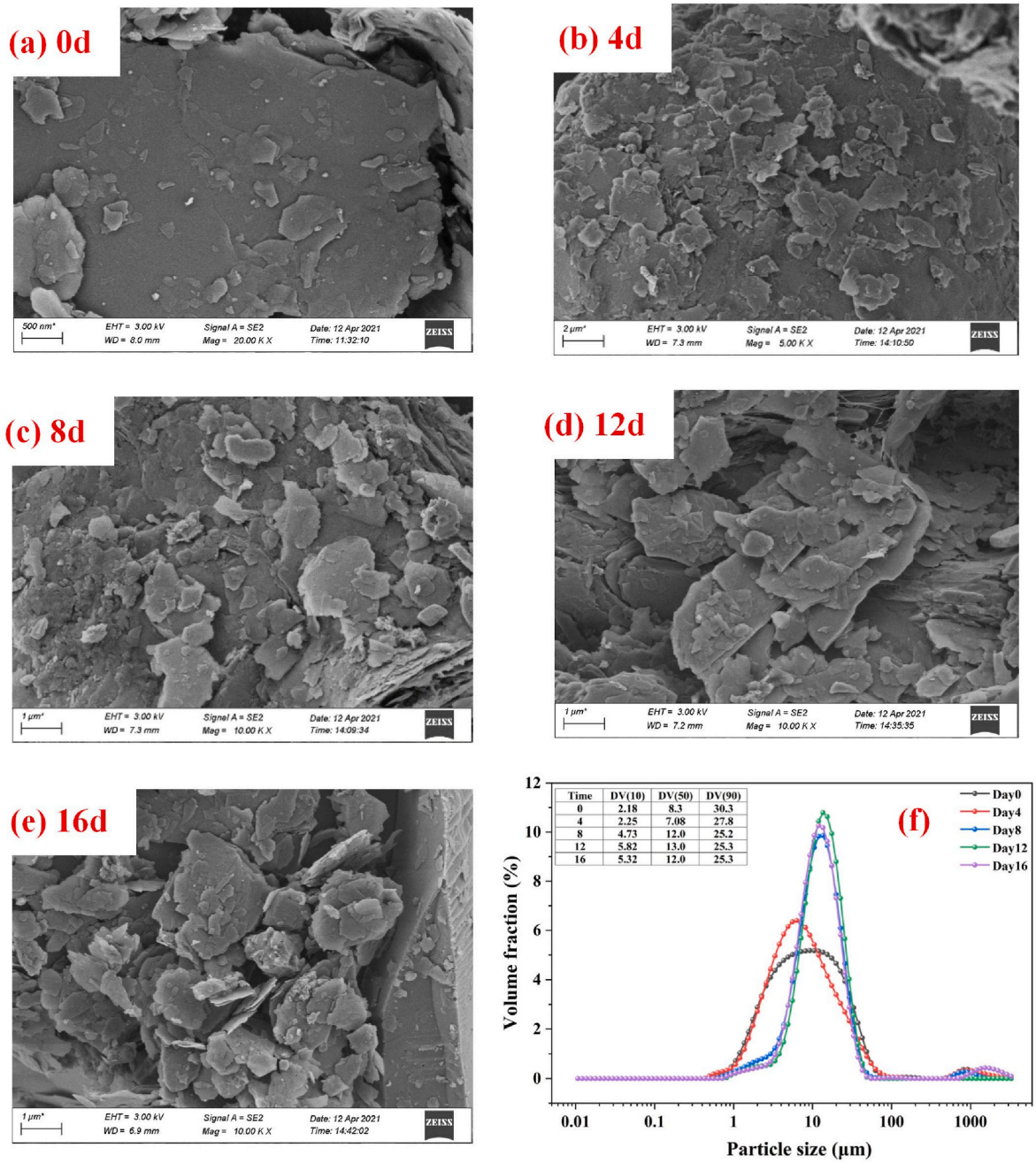

Fig. 5. (a)–(e) SEM images of fine sulfide raw ore at different leaching times, (f) Particle size distribution of fine sulfide raw ore with different leaching times.

ores. Microorganisms commonly attach in corrosion pits or grooves, benefitting the preferential oxidation of the edge erosion area of microorganisms (Ndlovu and Monhemius, 2005). EPS was produced when microorganisms attached to the mineral surface, facilitating the gathering of fine ores.

In addition, the variations in particle size distribution further illustrated the gathering phenomenon (Fig. 5(f)). DV(10), DV(50) and DV (90) (volume median diameter) represent the size below which 10, 50 and 90%, respectively, of the sample volume exists. Fine sulfide ore continually dissolved in 4 days, due to oxidation by microorganisms; this represented a declining trend in the DV(90) and DV(50). However, the particle size distribution of DV(50) and DV(10) increased after 8 days. These results indicated that the volume fraction of smaller fine ores decreased, while the volume fraction of bigger fine ores increased during the late stage. This illustrated the gathering action of fine sulfide ores, confirming the SEM results.

4. Conclusions

A novel designed moderately thermophilic consortia (*L. ferriphilum*+*A. caldus*+*S. benefaciens*) had a high level of microbial activity and achieved a leaching environment at a high oxidation-reduction potential and low pH, which benefits the oxidation of fine lead-zinc sulfide raw ore. These consortia realized a zinc extraction rate of up to 96.44% after 8 days and 100% after 12 days. Polysaccharides, EPS level, and amino acids of the consortia mainly affected the bioleaching of this fine sulfide raw ore. The mineral surface analysis showed that no jarosite was formed to hinder the bioleaching process at a low pH in the leaching system. The novel designed moderately thermophilic consortia was able to recover valuable metals in the minerals,

reducing potential pollution by the minerals. In summary, this research expands the opportunities available to apply bioleaching to treat unwieldy fine sulfide ore.

Credit author statement

Siyu Zhou: Conceptualization, Experiment, Data curation, Writing-Original draft preparation. Xiaojian Liao: Methodology, Writing-Reviewing and Editing. Shoupeng Li: Data curation. Xiaodi Fang：Experiment. Zhijie Guan and Maoyou Ye: Supervision, Investigation. Shuiyu Sun: Methodology, Funding acquisition. All authors discussed the results and contributed to the final manuscript.

Declaration of competing interest

The authors declare that they have no known competing financial interests or personal relationships that could have appeared to influence the work reported in this paper.

Acknowledgement

This work was supported by National Key R&D Program of China (No. 2018YFD0800700), Science and Technology Planning Project of Guangdong Province (No. 2016A040403068) and Natural Science Foundation of Guangdong Province (No. 2015A030308008). The authors also thank Shiyanjia Lab (www.shiyanjia.com) for support with the SEM test.

References

Ahmadi, A., Mousavi, S.J., 2015. The influence of physicochemical parameters on the bioleaching of zinc sulfide concentrates using a mixed culture of moderately thermophilic microorganisms. Int. J. Miner. Process. 135, 32–39.
Bryan, C.G., et al., 2011. The efficiency of indigenous and designed consortia in bioleaching stirred tank reactors. Miner. Eng. 24, 1149–1156.
Cai, P., et al., 2018. EPS adsorption to goethite: molecular level adsorption mechanisms using 2D correlation spectroscopy. Chem. Geol. 494, 127–135.
Castro, C., et al., 2019. Metal biorecovery and bioremediation: whether or not thermophilic are better than mesophilic microorganisms. Bioresour. Technol. 279, 317–326.
Castro, L., et al., 2013. Effectiveness of anaerobic iron bio-reduction of jarosite and the influence of humic substances. Hydrometallurgy 131–132, 29–33.
Chen, W., et al., 2003. Fluorescence excitation - emission matrix regional integration to quantify spectra for dissolved organic matter. Environ. Sci. Technol. 37, 5701–5710.
Chu, H., et al., 2021. Generation behavior of extracellular polymeric substances and its correlation with extraction efficiency of valuable metals and change of process parameters during bioleaching of spent petroleum catalyst. Chemosphere 275, 130006.
Feng, S., et al., 2016. Insights to the effects of free cells on community structure of attached cells and chalcopyrite bioleaching during different stages. Bioresour. Technol. 200, 186–193.
Feng, S., et al., 2021. Simultaneously enhance iron/sulfur metabolism in column bioleaching of chalcocite by pyrite and sulfur oxidizers based on joint utilization of waste resource. Environ. Res. 194, 110702.
Flemming, H.-C., Wingender, J., 2010. The biofilm matrix. Nat. Rev. Microbiol. 8, 623–633.
Gan, M., et al., 2015. Bioleaching of multiple heavy metals from contaminated sediment by mesophile consortium. Environ. Sci. Pollut. Res. Int. 22, 5807–5816.
Gu, T., et al., 2018. Advances in bioleaching for recovery of metals and bioremediation of fuel ash and sewage sludge. Bioresour. Technol. 261, 428–440.
Guo, L., et al., 2014. Three-dimensional fluorescence excitation-emission matrix (EEM) spectroscopy with regional integration analysis for assessing waste sludge hydrolysis treated with multi-enzyme and thermophilic bacteria. Bioresour. Technol. 171, 22–28.
Han, F., et al., 2018. Performance, microbial community and fluorescent characteristic of microbial products in a solid-phase denitrification biofilm reactor for WWTP effluent treatment. J. Environ. Manag. 227, 375–385.
He, Z.-g., et al., 2014. Effect of pyrite, elemental sulfur and ferrous ions on EPS production by metal sulfide bioleaching microbes. Trans. Nonferrous Metals Soc. China 24, 1171–1178.
Huang, Z., et al., 2019. Enhanced "contact mechanism" for interaction of extracellular polymeric substances with low-grade copper-bearing sulfide ore in bioleaching by moderately thermophilic Acidithiobacillus caldus. J. Environ. Manag. 242, 11–21.
Jiang, K.-q., et al., 2012. Effect of moderately thermophilic bacteria on metal extraction and electrochemical characteristics for zinc smelting slag in bioleaching system. Trans. Nonferrous Metals Soc. China 22, 3120–3125.
Kaksonen, A.H., et al., 2020. Acid and ferric sulfate bioleaching of uranium ores: a review. J. Clean. Prod. 264, 121586.
Koukal, B., et al., 2003. Influence of humic substances on the toxic effects of cadmium and zinc to the green alga Pseudokirchneriella subcapitata. Chemosphere 53, 953–961.
Li, Q., Sand, W., 2017. Mechanical and chemical studies on EPS from Sulfobacillus thermosulfidooxidans: from planktonic to biofilm cells. Colloids Surf. B Biointerfaces 153, 34–40.
Liao, X., et al., 2019. A new strategy on biomining of low grade base-metal sulfide tailings. Bioresour. Technol. 294, 122187.
Liao, X., et al., 2021. Simultaneous recovery of valuable metal ions and tailings toxicity reduction using a mixed culture bioleaching process. J. Clean. Prod. 316, 128319.
Liu, R., et al., 2020. Selective removal of cobalt and copper from Fe (III)-enriched high-pressure acid leach residue using the hybrid bioleaching technique. J. Hazard. Mater. 384, 121462.
Ma, L., et al., 2017. Co-culture microorganisms with different initial proportions reveal the mechanism of chalcopyrite bioleaching coupling with microbial community succession. Bioresour. Technol. 223, 121–130.
Mahmoud, A., et al., 2017. A review of sulfide minerals microbially assisted leaching in stirred tank reactors. Int. Biodeterior. Biodegrad. 119, 118–146.
Mangold, S., et al., 2011. Sulfur metabolism in the extreme acidophile *Acidithiobacillus caldus*. Front. Microbiol. 2, 17.
Mendez-Garcia, C., et al., 2015. Microbial diversity and metabolic networks in acid mine drainage habitats. Front. Microbiol. 6, 475.
Mikhlin, Y., et al., 2016. Ultrafine particles derived from mineral processing: a case study of the Pb-Zn sulfide ore with emphasis on lead-bearing colloids. Chemosphere 147, 60–66.
Nancucheo, I., Johnson, D.B., 2010. Production of glycolic acid by chemolithotrophic iron- and sulfur-oxidizing bacteria and its role in delineating and sustaining acidophilic sulfide mineral-oxidizing consortia. Appl. Environ. Microbiol. 76, 461–467.
Ndlovu, S., Monhemius, A.J., 2005. The influence of crystal orientation on the bacterial dissolution of pyrite. Hydrometallurgy 78, 187–197.
Nguyen, T.H., et al., 2021. Bioleaching for environmental remediation of toxic metals and metalloids: a review on soils, sediments, and mine tailings. Chemosphere 282.
Novikova, S.P., Gas'kova, O.L., 2013. Influence of natural fulvic acids on the solubility of sulfide ores (experimental study). Russ. Geol. Geophys. 54, 509–517.
Panda, S., et al., 2015. Current scenario of chalcopyrite bioleaching: a review on the recent advances to its heap-leach technology. Bioresour. Technol. 196, 694–706.
Priya, A., Hait, S., 2018. Extraction of metals from high grade waste printed circuit board by conventional and hybrid bioleaching using Acidithiobacillus ferrooxidans. Hydrometallurgy 177, 132–139.
Srichandan, H., et al., 2019. Bioleaching approach for extraction of metal values from secondary solid wastes: a critical review. Hydrometallurgy 189.
Sun, H., et al., 2015. Study of the kinetics of pyrite oxidation under controlled redox potential. Hydrometallurgy 155, 13–19.
Wang, X., et al., 2018a. Synergetic effect of pyrite on strengthening bornite bioleaching by *Leptospirillum ferriphilum*. Hydrometallurgy 176, 9–16.
Wang, J., et al., 2018b. Functional exploration of extracellular polymeric substances (EPS) in the bioleaching of obsolete electric vehicle LiNixCoyMn1-x-yO2 Li-ion batteries. J. Hazard. Mater. 354, 250–257.
Wang, Z.P., Zhang, T., 2010. Characterization of soluble microbial products (SMP) under stressful conditions. Water Res. 44, 5499–5509.
Wei, D., et al., 2017. Qualitative and quantitative analysis of extracellular polymeric substances in partial nitrification and full nitrification reactors. Bioresour. Technol. 240, 171–176.
Wong, J.W.C., et al., 2015. Influence of ferrous ions on extracellular polymeric substances content and sludge dewaterability during bioleaching. Bioresour. Technol. 179, 78–83.
Xiao, K., et al., 2016. Characterization of key organic compounds affecting sludge dewaterability during ultrasonication and acidification treatments. Water Res. 105, 470–478.
Xiao, N., et al., 2019. Effect of humic acid on photofermentative hydrogen production of volatile fatty acids derived from wastewater fermentation. Renew. Energy 131, 356–363.
Xie, Y., et al., 2017. Fulvic acid induced the liberation of chromium from CrO42−-substituted schwertmannite. Chem. Geol. 475, 52–61.
Xu, H., et al., 2013. Insights into extracellular polymeric substances of cyanobacterium Microcystis aeruginosa using fractionation procedure and parallel factor analysis. Water Res. 47, 6.1–6.10.
Xue, J., et al., 2021. Hydrophobic agglomeration flotation of oxidized digenite fine particles induced by Na2S and butyl xanthate. Miner. Eng. 168.
Ye, M., et al., 2017a. Bioleaching combined brine leaching of heavy metals from lead-zinc mine tailings: transformations during the leaching process. Chemosphere 168, 1115–1125.
Ye, M., et al., 2017b. Removal of metals from lead-zinc mine tailings using bioleaching and followed by sulfide precipitation. Chemosphere 185, 1189–1196.
Ye, M., et al., 2021. Bioleaching for detoxification of waste flotation tailings: relationship between EPS substances and bioleaching behavior. J. Environ. Manag. 279, 111795.
Yin, L., et al., 2020. Interfacial alteration of pyrite caused by bioleaching. Hydrometallurgy 195, 105356.
Yu, Z.-j., et al., 2017. Effect of pH values on extracellular protein and polysaccharide secretions of Acidithiobacillus ferrooxidans during chalcopyrite bioleaching. Trans. Nonferrous Metals Soc. China 27, 406–412.
Zahiri, A., et al., 2021. Improvement of zinc bioleaching from a zinc flotation concentrate using mechanical activation. Miner. Eng. 163 (2), 106793.

Zhang, S., et al., 2019. Analysis of the relationship of extracellular polymeric substances to the dewaterability and rheological properties of sludge treated by acidification and anaerobic mesophilic digestion. J. Hazard. Mater. 369, 31–39.
Zhao, H., et al., 2015. Effect of redox potential on bioleaching of chalcopyrite by moderately thermophilic bacteria: an emphasis on solution compositions. Hydrometallurgy 151, 141–150.
Zhao, J., et al., 2019. Accelerated productions and physicochemical characterizations of different extracellular polymeric substances from Chlorella vulgaris with nano-ZnO. Sci. Total Environ. 658, 582–589.
Zhu, J., et al., 2015. Insights into the relation between adhesion force and chalcopyrite-bioleaching by Acidithiobacillus ferrooxidans. Colloids Surf. B Biointerfaces 126, 351–357.
Zhu, W., et al., 2013. Thermophilic archaeal community succession and function change associated with the leaching rate in bioleaching of chalcopyrite. Bioresour. Technol. 133, 405–413.